E-5-2

Extended Abstracts of the 2011 International Conference on Solid State Devices and Materials, Nagoya, 2011, pp917-918

Improvement of Thermal stability of Ni-Germanide with Ni/Co/Ni/TiN Structure for High Performance Ge MOSFETs

Hong-Sik Shin[1], Se-Kyung Oh[1] , Min-Ho Kang[1,2] , Hyuk-Min Kwon[1], Jungwoo Oh[3], Prashant Majhi[3], Raj Jammy[3], Ga-Won Lee[1] and Hi-Deok Lee[1,*]

[1] Dept. of Electronics Engineering, Chungnam National University, Gung-Dong, Yuseong, Daejeon 305-764, Korea
Tel. +82-42-821-7702, Fax. +82-42-823-9544, *E-mail: hdlee@cnu.ac.kr
[2] Division of Nano-Process Technology, National NanoFab Center (NNFC), Daejeon, 305-806, Korea
[3]SEMATECH, 2706 Montopolis Drive, Austin, TX 78741 USA

1. Introduction

The higher mobility of carriers in germanium (Ge) compared to silicon (Si) counterpart that is two times for electrons and four times for holes, has received a lot of interest for Ge metal oxide semiconductor field effect transistors (Ge MOSFETs) [1-3]. Self-aligned germanide (Salmanide) technology, like self-aligned silicide (Salicide) technology [4], is also highly necessary as contact metallization materials for high performance Ge MOSFETs. Ni germanide is the most popular due to its advantage over Ti and Co germanide, such as its low formation temperature (> 250 ^{o}C), its stable phase over wide temperature range (NiGe) and its low resistivity (22 μΩcm) [5]. However, its poor thermal stability should be improved for application to Ge MOSFETs [6-9]. Therefore, improvement of the thermal stability is inevitable for developing salmanide technology for Ge MOSFETs. In this paper, Ni/Co/Ni/TiN structure is proposed to improve the thermal stability of Ni germanide on Ge-on-Si substrate.

2. Experiments

Process flow for experiments is summarized in Fig. 1. A 100 nm thick Ge layer is deposited on 8” silicon substrate (Ge-on-Si structure) using an ultra-high vacuum chemical vapor deposition (UHV-CVD) method. Ge-on-Si substrate was cleaned with dilute hydrofluoric acid (HF: H_2O=1: 100) solution. Ni/TiN (15/10 nm) and Ni/Co/Ni/TiN (10/2/3/l0 nm) was deposited subsequently by using RF magnetron sputtering system. After formation of NiGe by using one step rapid thermal process (RTP) from 300 to 700 ^{o}C for 30 sec, the unreacted metal and TiN layer were etched away using phosphoric acid (H_3PO_4) solution at 150 ^{o}C for 30 sec. To evaluate the thermal stability of the fabricated NiGe film, a post-germanidation annealing was carried from 500 to 600 ^{o}C for 30 min. Reference Ni/TiN (15/10 nm) was also prepared for comparison.

3. Results and discussion

Figure 2 shows a sheet resistance of NiGe on Ge-on-Si substrate as a function of RTP temperature for pure Ni and Ni/Co/Ni/TiN structures. It can be seen that sheet resistance of pure Ni structure drops at 300 ^{o}C, indicating the formation of NiGe while that of Ni/Co/Ni/TiN structure becomes low at 400 ^{o}C. Sheet resistance of pure Ni structure begins to increase from 600 ^{o}C, while that of Ni/Co/Ni/TiN structure begins to increase from 650 ^{o}C. We can also find that Ni/Co/Ni/TiN structure has the higher sheet resistance than the Ni/TiN case.

The dependence of the NiGe sheet resistance on post-germanidation annealing temperature is shown in Fig. 3. Sheet resistance of Ni/TiN structure begins to increase by post-germanidation annealing from 500 ^{o}C, while Ni/Co/Ni/TiN structure begins to increase from 550 ^{o}C. The sharp increase in resistance can be attributed to agglomeration and/or penetration of NiGe.

Figure 4 shows the cross-sectional FE-SEM images of Ni germanide after 400 °C RTP and 550 °C annealing. Although there is little difference in the germanide profile between Ni/TiN and Ni/Co/Ni/TiN structures just after RTP, Ni/TiN shows severe agglomeration after post-germanidation annealing at 500 °C for 30 min as shown in Fig. 4 (c). However, the proposed Ni/Co/Ni/TiN structure exhibits uniform germanide/Ge interface even for the 550^{o}C annealing shown in Fig. 4 (d).

SIMS depth profile of NiGe after 550 °C post-germanidation annealing was investigated to compare the NiGe profile as shown in Fig. 5. Ni/TiN structure shows a wide distribution of Ni in the Ge layer, while Ni/Co/Ni/TiN exhibits a sharp distribution of Ni at the top region of the Ge layer, meaning uniform formation of NiGe as shown in Fig. 5 (a) and (b), respectively. Moreover, in the case of the Ni/Co/Ni/TiN structure, there is an increase in Co elements at the interface of NiGe/Ge. While part of this could certainly be a matrix effect at the interface, the presence of Co at this point could explain the delay in morphological degradation. Therefore, Addition of ultrathin Co layer can improve the thermal stability of NiGe, which is due to the retarded agglomeration of Nigermanide.

Figure 6 shows the cross-sectional HR FETEM images (Corresponding HR FETEM EDS analysis) of NiGe after 550°C post-germanidation annealing. It is clear that the Ni/TiN structure shows agglomeration, while the Ni/Co/Ni/TiN structure exhibits a uniform interface.

4. Conclusions

Thermal stability of NiGe is improved by the proposed Ni/Co/Ni/TiN structure with the Cobalt incorporation into the Nigermanide. The proposed Ni/Co/Ni/TiN structure is promising for highly thermal immune Nigermanide for high performance Ge MOSFETs.

Acknowledgements

This work was supported in part by grant No. 2009-0069103 from the Korea Science and Engineering Foundation (KOSEF). This work was also financially supported in part by the Ministry of Knowledge Economy (MKE) and Korea Industrial Technology Foundation (KOTEF) through the Human Resource Training Project for Strategic Technology. The authors thank the Busan centers of the Korea Basic Science Institute for SIMS (model: CAMECA IMS-6f) analyses.

References

[1] N. Wu et al., IEEE Trans. Electron Device. **54** (2007) 733.
[2] J. W. Oh et al., Electron Device Lett., **28** (2007) 1044.
[3] T. Tezuka, et al., Symposium on VLSI Technology Digest (2002) 96.
[4] R. Li, et al., Thin Solid Films **504** (2006) 28.
[5] S. Gaudeta et al., J, Vac. Sci. Technol. A24 (2005) 464.
[6] Y. Zhang et al., IEEE Trans. Electron Devices **56** (2009) 348.
[7] Y. Zhang et al., Electrochem. Solid State Lett. **12** (2009) H402.
[8] S. Zhu et al., Jpn. J. Appl. Phys. **44** (2005) L753.
[9] K. Park et al., Electrochem. Solid State Lett. **154** (2007) H557

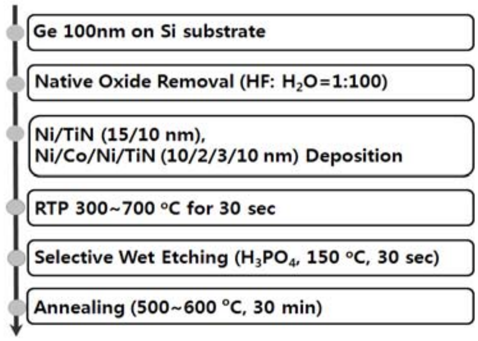

Fig. 1 Key process flow for experiments. Ni germanide is formed on the 1000 Å thick Ge-on-Si substrate.

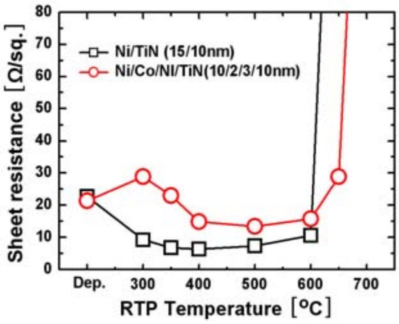

Fig. 2. Sheet resistance of Ni germanide as a function of RTP temperature for 30 sec.

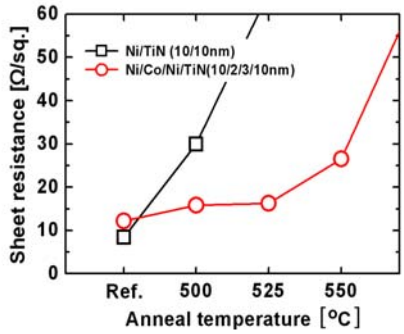

Fig. 3. Sheet resistance of Ni germanide as a function of annealing temperature for 30 min.

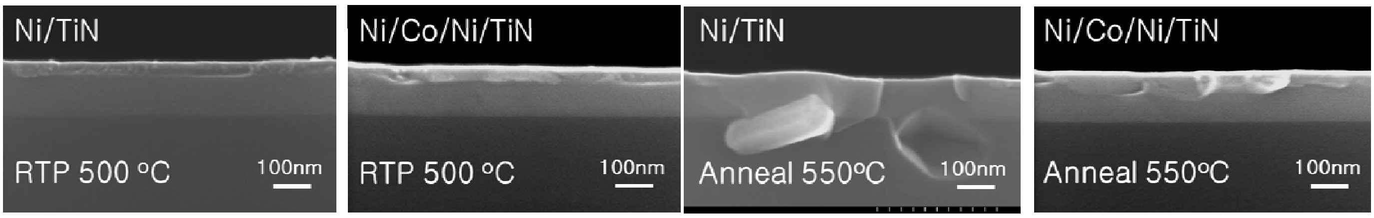

(a) (b) (c) (d)

Fig. 4. Cross-sectional FE-SEM images of Ni germanide. (a), (c) Ni/TiN and (b), (d) Ni/Co/TiN structures. (a) and (b) are after RTP at 500°C for 30 sec and (c) and (d) are after annealing at 550°C for 30 min.

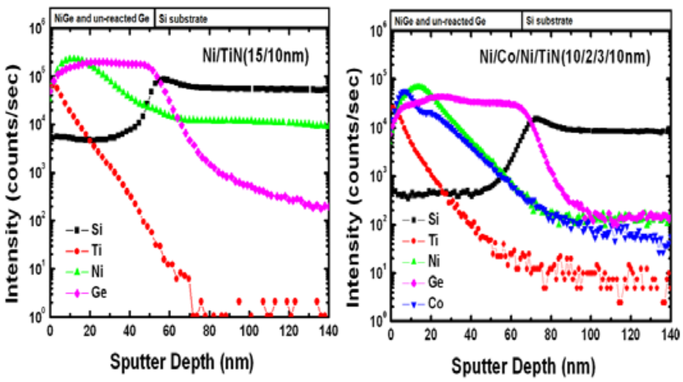

(a) (b)

Fig. 5. SIMS depth profiles of Ni germanide for (a) Ni/TiN and (b) Ni/Co/Ni/TiN structures after post-germanidation annealing at 550°C.

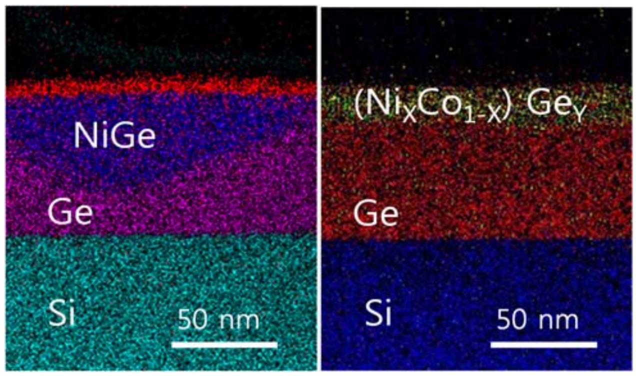

(a) (b)

Fig. 6. Cross-sectional HR FETEM images of NiGe for (a) Ni/TiN and (b) Ni/Co/Ni/TiN structures after post-germanidation annealing at 550°C. (Corresponding HR FETEM EDS analysis.)